

# THE RATIONAL SPDE APPROACH FOR GAUSSIAN RANDOM FIELDS WITH GENERAL SMOOTHNESS

DAVID BOLIN AND KRISTIN KIRCHNER

*Department of Mathematical Sciences  
Chalmers University of Technology and University of Gothenburg  
412 96 Göteborg, Sweden*

ABSTRACT. A popular approach for modeling and inference in spatial statistics is to represent Gaussian random fields as solutions to stochastic partial differential equations (SPDEs) of the form  $L^\beta u = \mathcal{W}$ , where  $\mathcal{W}$  is Gaussian white noise,  $L$  is a second-order differential operator, and  $\beta > 0$  is a parameter that determines the smoothness of  $u$ . However, this approach has been limited to the case  $2\beta \in \mathbb{N}$ , which excludes several important covariance models and makes it necessary to keep  $\beta$  fixed during inference.

We introduce a new method, the rational SPDE approach, which is applicable for any  $\beta > 0$  and therefore remedies the mentioned limitation. The presented scheme combines a finite element discretization in space with a rational approximation of the function  $x^{-\beta}$  to approximate  $u$ . For the resulting approximation, an explicit rate of strong convergence to  $u$  is derived and we show that the method has the same computational benefits as in the restricted case  $2\beta \in \mathbb{N}$  when used for statistical inference and prediction. Several numerical experiments are performed to illustrate the accuracy of the method, and to show how it can be used for likelihood-based inference for all model parameters including  $\beta$ .

## 1. INTRODUCTION

One of the main challenges in spatial statistics is to handle large data sets. A reason for this is that the computational cost for likelihood evaluation and spatial prediction is in general cubic in the number  $N$  of observations of a Gaussian random field. A tremendous amount of research has been devoted to coping with this problem and various methods have been suggested (see Heaton et al., 2017, for a recent review).

---

*E-mail address:* (D. Bolin, corresponding author) [david.bolin@chalmers.se](mailto:david.bolin@chalmers.se).

*Date:* July 19, 2022.

*2010 Mathematics Subject Classification.* Primary: 60G15, 62M09, 62M30, 65C30, 65C60.

*Key words and phrases.* fractional operators, Gaussian random fields, Matérn covariances, spatial statistics, stochastic partial differential equations.

This work has been supported in part by the Swedish Research Council under grant No. 2016-04187 and the Knut and Alice Wallenberg Foundation (KAW 20012.0067). The authors thank Stig Larsson and Finn Lindgren for valuable comments on the manuscript.

A common approach is to define an approximation  $u_h$  of the Gaussian field  $u$  on the domain  $\mathcal{D}$  via a basis expansion,

$$u_h(\mathbf{s}) = \sum_{i=1}^n u_i \varphi_i(\mathbf{s}), \quad \mathbf{s} \in \mathcal{D}, \quad (1.1)$$

where  $\{\varphi_i\} \subset L_2(\mathcal{D})$  are fixed basis functions and  $\mathbf{u} = (u_1, \dots, u_n)^\top \sim \mathbf{N}(\mathbf{0}, \boldsymbol{\Sigma}_u)$  are stochastic weights. The computational effort can then be reduced by choosing  $n \ll N$ , which is exploited in methods such as fixed-rank kriging (Cressie and Johannesson, 2008), predictive processes (Banerjee et al., 2008), and process convolutions (Higdon, 2002). However, methods based on such low-rank approximations tend to remove fine-scale variations of the process (Simpson et al., 2012; Bolin and Lindgren, 2013).

For this reason, methods which instead exploit sparsity for reducing the computational cost have gained popularity in recent years. One can construct sparse approximations either of the covariance matrix of the measurements, as for covariance tapering approximations (Furrer et al., 2006), or of the inverse of the covariance matrix (the precision matrix), as for nearest neighbor process approximations (Datta et al., 2016). Alternatively, one can let the precision matrix  $\boldsymbol{\Sigma}_u^{-1}$  of the weights in (1.1) be sparse, as in the stochastic partial differential equation (SPDE) approach (Lindgren et al., 2011). This tends to perform better than the low-rank approach, but since the true model typically has neither a sparse covariance matrix nor a sparse precision matrix, there is naturally a limit to how accurate these approximations can be, if a given sparsity should be achieved.

Another idea for reducing the computing time is to include parallelization, such as for subsampling (Barbian and Assunção, 2017) or domain decompositions (Sang et al., 2011), and there are several methods which combine the mentioned approaches to increase the accuracy. For example, Nychka et al. (2015a) use a multiresolution basis  $\{\varphi_i\}$ , where every level of the basis has a sparse precision matrix. Multiresolution bases can also be combined with the predictive process approach, covariance tapering, or domain partitioning as in (Katzfuss, 2017). Empirically, the multiresolution approaches seem to work well, see, for instance, the comparison in (Heaton et al., 2017). However, to the best of our knowledge, no theoretical error bounds have been derived, which necessitates tuning of these methods for each specific model.

In this work we propose a new class of approximations, which we refer to as rational (SPDE) approximations. Our approach is similar to some of the above methods in the sense that a basis expansion (1.1) with compactly supported basis functions is exploited. The main novelty is that neither the covariance matrix  $\boldsymbol{\Sigma}_u$  nor the precision matrix  $\boldsymbol{\Sigma}_u^{-1}$  of the weights  $\mathbf{u}$  are assumed to be sparse. The covariance matrix is instead a product  $\boldsymbol{\Sigma}_u = \mathbf{P}_r \mathbf{Q}^{-1} \mathbf{P}_r^T$ , where  $\mathbf{P}_r$  and  $\mathbf{Q}$  are sparse matrices and the sparsity pattern of  $\mathbf{P}_r$  is a subset of the sparsity pattern of  $\mathbf{Q}$ . We show that the resulting approximation facilitates inference and prediction at the same computational cost as a Markov approximation with  $\boldsymbol{\Sigma}^{-1} = \mathbf{Q}$ , and at a higher accuracy. The reason for this beneficial behavior is similar to why, in the time series literature, ARMA approximations are often more accurate than AR approximations.

For the theoretical framework of our approach, we consider a Gaussian random field on a bounded domain  $\mathcal{D} \subset \mathbb{R}^d$  which can be represented as the solution  $u$  to

the SPDE

$$L^\beta u = \mathcal{W} \quad \text{in } \mathcal{D}, \quad (1.2)$$

where  $\mathcal{W}$  is Gaussian white noise, and  $L^\beta$  is a fractional power of a second-order differential operator which determines the covariance function of  $u$ . The method for calculating the rational approximation is based on two components: (i) a finite element method (FEM) in space with continuous piecewise polynomial basis functions  $\{\varphi_i\}$  defined with respect to a regular triangulation of  $\mathcal{D}$ , and (ii) a rational approximation of the function  $x^{-\beta}$ . We show how to perform these two steps in practice in order to explicitly compute the matrices  $\mathbf{P}_r$  and  $\mathbf{Q}$ . Furthermore, we derive an upper bound for the strong mean-square error of the rational approximation. This bound provides an explicit rate of convergence in terms of the mesh size of the finite element discretization, which facilitates choosing the approximation based on theoretical arguments instead of using empirical tests for each specific model.

Examples of random fields which can be expressed as solutions to SPDEs of the form (1.2) include approximations of Gaussian Matérn fields (Matérn, 1960). Specifically, if  $\mathcal{D} := \mathbb{R}^d$  is the whole space, a mean-zero Gaussian Matérn field can be viewed as the stationary solution,  $u$ , to the SPDE

$$(\kappa^2 - \Delta)^\beta (\tau u) = \mathcal{W}, \quad (1.3)$$

where  $\Delta$  denotes the Laplacian (Whittle, 1963). The constant parameters  $\kappa, \tau > 0$  determine the practical correlation range and the variance of  $u$ , respectively. The exponent  $\beta$  defines the smoothness parameter  $\nu$  of the Matérn covariance function via the relation  $2\beta = \nu + d/2$  and, thus, the differentiability of the field. In contrast to covariance-based models, this representation has the advantage that it allows for a number of generalizations of stationary Matérn fields including (i) non-stationary fields obtained by considering more general differential operators (Fuglstad et al., 2015; Lindgren et al., 2011), (ii) fields on more general domains such as the sphere (Bolin and Lindgren, 2011; Lindgren et al., 2011), and (iii) non-Gaussian Matérn fields (Bolin, 2014; Wallin and Bolin, 2015).

Lindgren et al. (2011) showed that one can construct accurate approximations of Gaussian Matérn fields on bounded domains if  $2\beta \in \mathbb{N}$ . These approximations are of the form (1.1), where  $\Sigma_u^{-1}$  is sparse. For this, (1.3) is considered on a bounded domain  $\mathcal{D} \subsetneq \mathbb{R}^d$ , and the differential operator  $\kappa^2 - \Delta$  is augmented with homogeneous Neumann boundary conditions. The resulting stochastic problem is then solved approximately by means of a FEM. However, this approximation is only computable if  $2\beta \in \mathbb{N}$ , which limits the flexibility of the method. In particular, it can therefore not be applied to the important special case of exponential covariance on  $\mathbb{R}^2$ , where  $\beta = 3/4$ . In addition, the method requires a fixed value of  $\beta$  during inference. For this reason, the approach by Lindgren et al. (2011) cannot be used if the smoothness of the process has to be estimated from data. The rational SPDE approach presented in this work solves this issue by providing an approximation of  $u$  which is computable for all fractional powers  $\beta > 0$  and for both stationary Matérn fields as well as all generalizations named above.

The structure of this article is as follows: We briefly review existing methods for fractional SPDEs in §2. In §3 the rational SPDE approximation is introduced and a result on its strong convergence is stated. The procedure of using the rational SPDE approximation for statistical inference is addressed in §4. §5 contains several

numerical experiments which illustrate the accuracy of the proposed method and show how it can be used to perform likelihood-based inference of all parameters in the model including  $\beta$ . In §6 we present an application and compare the method to covariance tapering. The article concludes with a discussion in §7. Finally, this article contains three appendices providing details about (A) the finite element discretization, (B) the convergence analysis, and (C) the relation between the rational SPDE approach and the quadrature method by (Bolin et al., 2017).

The method developed in this work has been implemented in the R (R Core Team, 2017) package rSPDE (Bolin, 2017), which also includes code for replicating the results of the application considered in §6.

## 2. EXISTING APPROXIMATION METHODS FOR FRACTIONAL SPDES

A reason for why the approach by Lindgren et al. (2011) only works for integer values of  $2\beta$  is given by Rozanov (1977), who showed that a Gaussian random field on  $\mathbb{R}^d$  is Markov if and only if its spectral density can be written as the reciprocal of a polynomial,  $\tilde{S}(\mathbf{k}) = (\sum_{j=0}^m b_j \|\mathbf{k}\|^{2j})^{-1}$ . Since the spectrum of a Gaussian Matérn field is

$$S(\mathbf{k}) = \frac{1}{(2\pi)^d} \frac{1}{(\kappa^2 + \|\mathbf{k}\|^2)^{2\beta}}, \quad \mathbf{k} \in \mathbb{R}^d, \quad (2.1)$$

the precision matrix  $\mathbf{Q}$  will therefore not be sparse unless  $2\beta \in \mathbb{N}$ . For  $2\beta \notin \mathbb{N}$ , Lindgren et al. (2011) suggested to compute a Markov approximation by choosing  $m = \lceil 2\beta \rceil$  and selecting the coefficients  $\mathbf{b} = (b_1, \dots, b_m)^\top$  so that the deviation between the spectral densities  $\int_{\mathbb{R}^d} w(\mathbf{k})(S(\mathbf{k}) - \tilde{S}(\mathbf{k}))^2 d\mathbf{k}$  is minimized. For this measure of deviation,  $w$  is some suitable weight function which should be chosen to get a good approximation of the covariance function. For the method to be useful in practice, the coefficients  $b_j$  should be given explicitly in terms of the parameters  $\kappa$  and  $\nu$ . Because of this, Lindgren et al. (2011) proposed a weight function that enables an analytical evaluation of the integral,

$$\int_{\kappa^2}^{\infty} \left[ z^{2\beta} - \sum_{j=0}^m b_j (z - \kappa^2)^j \right]^2 z^{-2m-1-\theta} dz,$$

where  $\theta > 0$  is a tuning parameter. By differentiating the integral with respect to the parameters and setting the differentials equal to zero, a system of linear equations is obtained, which can be solved to find the coefficients  $\mathbf{b}$ . The resulting approximation depends strongly on  $\theta$ , and one could use numerical optimization to find a good value of  $\theta$  for a specific value of  $\beta$ , or use the choice  $\theta = 2\beta - \lceil 2\beta \rceil$ , which approximately minimizes the maximal distance between the covariance functions (Lindgren et al., 2011). This method was used for the comparison in (Heaton et al., 2017), and we will use it as a baseline method when analyzing the accuracy of the rational SPDE approximations in later sections.

Another Markov approximation based on the spectral density was proposed by Roininen et al. (2017). These Markov approximations may be sufficient in certain applications; however, since the Gaussian Matérn fields are not Markov unless  $2\beta \in \mathbb{N}$ , there is a natural limit to how precise they can be. In addition, any approach based on the spectral density or the covariance function is difficult to generalize to models on more general domains than  $\mathbb{R}^d$ , non-stationary models, or non-Gaussian models. Thus, such methods cannot be used if the full potential of the SPDE approach should be kept for fractional values of  $\beta$ .

There is a rich literature on methods for solving deterministic fractional PDEs (e.g., Baeumer et al., 2015; Bonito et al., 2017; Bonito and Pasciak, 2015; Caffarelli and Silvestre, 2007; Gavriluk, 1996; Gavriluk et al., 2004, 2005; Jin et al., 2015; Nochetto et al., 2015; Roop, 2006), and some of the methods that have been proposed could be used to compute approximations of the solution to the SPDE (1.3). However, any deterministic problem becomes more sophisticated when randomness is included. Furthermore, for making the approach attractive for statistical applications, the proposed scheme has to be very efficient, since likelihood evaluations, spatial predictions, and posterior sampling are often needed. Even methods developed specifically for sampling SPDEs like (1.3) may be too computationally demanding to be used for statistical inference. We will illustrate this by comparing the rational SPDE approach introduced in this work to the method proposed by Bolin et al. (2017), which is based on a quadrature approximation of an integral representation of the inverse fractional power operator: we compare their performance in practice within the scope of a numerical experiment in §5.1 and present similarities and differences of the approaches with respect to the theoretical derivation in Appendix C.

### 3. RATIONAL APPROXIMATIONS FOR FRACTIONAL SPDES

In this section we propose an explicit scheme for approximating solutions to a class of SPDEs including (1.3). Specifically, in §3.1 we introduce the fractional order equation of interest as well as its finite element discretization in space. In §3.2 we propose a non-fractional equation, whose solution after specification of certain coefficients approximates the random field of interest. This approximation is justified in theory in §3.3. Finally, in §3.4 we address the computation of the coefficients in the rational approximation.

**3.1. The fractional order equation.** In order to allow for more general Gaussian fields than the Matérn fields, we consider the fractional order equation (1.2) where  $\mathcal{D} \subset \mathbb{R}^d$ ,  $d \in \{1, 2, 3\}$ , is a bounded, convex, polygonal domain, and  $\mathcal{W}$  is Gaussian white noise on  $\mathcal{D}$ . The operator  $L: \mathcal{D}(L) \subset L_2(\mathcal{D}) \rightarrow L_2(\mathcal{D})$  is supposed to be a densely defined, self-adjoint, positive definite linear differential operator of second order, with a compact inverse. On the boundary  $\partial\mathcal{D}$ , homogeneous Dirichlet or Neumann boundary conditions are imposed on the operator, and depending on the boundary conditions we either set  $V := H_0^1(\mathcal{D})$  or  $V := H^1(\mathcal{D})$ . Furthermore, we assume that there exist constants  $A \geq a > 0$  such that

$$\langle Lw, v \rangle \leq A \|w\|_{H^1(\mathcal{D})} \|v\|_{H^1(\mathcal{D})}, \quad \langle Lv, v \rangle \geq a \|v\|_{H^1(\mathcal{D})}^2 \quad \forall w, v \in V.$$

Let  $V^*$  be the dual space of  $V$  after identifying functionals  $g: V \rightarrow \mathbb{R}$  via the Riesz map on  $L_2(\mathcal{D})$ . We denote the duality pairing between  $g \in V^*$  and  $\psi \in V$  by  $\langle g, \psi \rangle$ , and the inner product on  $L_2(\mathcal{D})$  by  $(\cdot, \cdot)_{L_2(\mathcal{D})}$ . Note that the operator  $L$  defined on  $\mathcal{D}(L) \subset V$  has a unique continuous extension to a bounded linear operator  $L: V \rightarrow V^*$  (cf. Lemma 2.1 of Bolin et al., 2017).

In order to discretize the problem, we assume that  $V_h \subset V$  is a finite element space with continuous piecewise polynomial basis functions  $\{\varphi_j\}_{j=1}^n$  of degree  $p \in \mathbb{N}$  defined with respect to a triangulation  $\mathcal{T}_h$  of the domain  $\mathcal{D}$  with mesh size  $h := \max_{T \in \mathcal{T}_h} \text{diam}(T)$ . Furthermore, the family  $(\mathcal{T}_h)_{h \in (0,1)}$  of triangulations inducing the finite-dimensional subspaces  $(V_h)_{h \in (0,1)}$  of  $V$  is supposed to be quasi-uniform.

The discretized operator  $L_h$  on  $V_h$  is defined in terms of  $L$  by

$$L_h: V_h \rightarrow V_h, \quad (L_h \psi_h, \phi_h)_{L_2(\mathcal{D})} = \langle L \psi_h, \phi_h \rangle \quad \forall \psi_h, \phi_h \in V_h.$$

We then consider the following SPDE with the state space  $V_h$ ,

$$L_h^\beta u_h = \mathcal{W}_h \quad \text{in } \mathcal{D}, \quad (3.1)$$

where  $\mathcal{W}_h$  is Gaussian white noise in  $V_h$ , i.e.,  $\mathcal{W}_h = \sum_{j=1}^{\dim(V_h)} \xi_j e_{j,h}$  for independent and identically  $\mathcal{N}(0,1)$ -distributed random variables  $\{\xi_j\}$  and a basis  $\{e_{j,h}\}$  of  $V_h$  that is orthonormal in  $L_2(\mathcal{D})$ .

In what follows, let  $\{\lambda_j\}_{j \in \mathbb{N}}$  and  $\{\lambda_{j,h}\}_{j=1}^n$  denote the positive eigenvalues of the operators  $L$  and  $L_h$ , respectively, which are listed in nondecreasing order. We suppose that the growth of the eigenvalues of  $L$  is given by  $\lambda_j \propto j^\alpha$ , i.e., there exists constants  $\alpha, c_\lambda, C_\lambda > 0$  such that

$$c_\lambda j^\alpha \leq \lambda_j \leq C_\lambda j^\alpha \quad \forall j \in \mathbb{N}. \quad (3.2)$$

We furthermore assume that the growth exponent  $\alpha > 0$  satisfies the following

$$\frac{1}{2\beta} \leq \alpha \leq \frac{2}{d}. \quad (3.3)$$

In this case, the Lemmas 2.8, 3.1, 3.2 of Bolin et al. (2017) provide an error estimate for the finite element approximation  $u_h = L_h^{-\beta} \mathcal{W}_h$  in (3.1) if  $\beta \in (0, 1)$ . Furthermore, since their derivation requires only that  $\beta$  is positive, we can formulate this result for all values  $\beta > 0$  in the following proposition.

**Proposition 3.1.** *Let  $u, u_h$  be the solutions to (1.2) and (3.1), respectively. Under the above assumptions, there exists a constant  $C > 0$ , independent of  $h$ , such that*

$$\|u - u_h\|_{L_2(\Omega; L_2(\mathcal{D}))} \leq Ch^{\min\{d(\alpha\beta-1/2), p+1\}}$$

holds for sufficiently small  $h$ .

**Example 3.2.** For the Matérn operator  $L = \kappa^2 - \Delta$ , the growth condition (3.2) is satisfied for  $\alpha = 2/d$ . Furthermore, (3.3) holds if  $\beta > d/4$ , which corresponds to a positive smoothness parameter  $\nu > 0$  of the field. The strong convergence rate of  $u_h$  is  $\min\{2\beta - d/2, p + 1\}$  in this case.

Since the mean-square error between  $u$  and  $u_h$  in  $L_2(\mathcal{D})$  converges to zero as  $h \rightarrow 0$ , it remains to describe how an approximation of the random field  $u_h$  with values in the finite-dimensional state space  $V_h$  can be constructed.

**3.2. The rational approximation.** For  $\beta \in \mathbb{N}$  one can use, e.g., the iterated finite element method presented in Appendix A to compute  $u_h$  in (3.1) directly. In the following, we construct approximations of  $u_h$  if  $\beta \notin \mathbb{N}$  is a fractional exponent. For this purpose, we aim at finding a non-fractional equation

$$P_{\ell,h} u_{h,m}^R = P_{r,h} \mathcal{W}_h \quad \text{in } \mathcal{D}, \quad (3.4)$$

such that  $u_{h,m}^R$  is a good approximation of  $u_h$ , and where the operator  $P_{j,h} := p_j(L_h)$  is defined in terms of a polynomial  $p_j$  of degree  $m_j$ ,  $j \in \{\ell, r\}$ . Comparing the initial equation (1.2) with

$$P_\ell u_m^R = P_r \mathcal{W} \quad \text{in } \mathcal{D}, \quad (3.5)$$

where  $P_j := p_j(L)$ ,  $j \in \{\ell, r\}$ , motivates the choice  $m_\ell - m_r \approx \beta$  in order to obtain a similar smoothness of  $u_m^R = (P_r^{-1}P_\ell)^{-1}\mathcal{W}$  and  $u = L^{-\beta}\mathcal{W}$  in (1.2). In practice, we set

$$m_r = m \in \mathbb{N} \quad \text{and} \quad m_\ell = m + m_\beta, \quad \text{where} \quad m_\beta := \max\{1, \lfloor \beta \rfloor\}. \quad (3.6)$$

In this case, the solution  $u_m^R$  of (3.5) has the same smoothness as the solution  $v$  of the non-fractional equation

$$\begin{cases} L^{\lfloor \beta \rfloor} v = \mathcal{W}, & \text{if } \beta \geq 1, \\ Lv = \mathcal{W}, & \text{if } \beta < 1, \end{cases}$$

and, for fixed  $h$ , the degree  $m$  controls the accuracy of the approximation  $u_{h,m}^R$ .

We now turn to the problem of selecting the non-fractional operators  $P_{\ell,h}$  and  $P_{r,h}$  in (3.4). In order to compute  $u_h$  in (3.1) directly, one would have to apply the discrete fractional inverse  $L_h^{-\beta}$  to the noise term  $\mathcal{W}_h$  on the right-hand side. Therefore, a first idea would be to approximate the function  $x^{-\beta}$  on the spectrum of  $L_h$  by a rational function  $\tilde{r}$  and to use  $\tilde{r}(L_h)\mathcal{W}_h$  as an approximation of  $u_h$ . This is, in essence, the approach proposed by Harizanov et al. (2016) to find optimal solvers for the problem  $\mathbf{L}^\beta \mathbf{x} = \mathbf{f}$ , where  $\mathbf{L}$  is a sparse symmetric positive definite matrix. However, the spectra of  $L$  and of  $L_h$  as  $h \rightarrow 0$  are unbounded and, thus, it would be necessary to normalize the spectrum of  $L_h$  for every  $h$ , since it is not feasible to construct the rational approximation  $\tilde{r}$  on an unbounded interval. A possible normalization  $\bar{L}_h$  of  $L_h$  is given by  $\bar{L}_h := \lambda_{\max,h}^{-1} L_h$ , where  $\lambda_{\max,h}$  is the largest eigenvalue of  $L_h$ . We then obtain  $L_h^{-\beta} \approx \lambda_{\max,h}^{-\beta} \tilde{r}(\bar{L}_h) = \tilde{r}_h(L_h)$ , i.e., the coefficients in the rational approximation  $\tilde{r}_h$ , which is applied to  $L_h$ , depend on  $\lambda_{\max,h}$ . Since we aim at an approximation  $L_h^{-\beta} \approx p_\ell(L_h)^{-1} p_r(L_h)$ , where in practice the coefficients of  $p_\ell$  and  $p_r$  can be made independent of  $L_h$  and  $h$ , we pursue another idea.

In contrast to the operator  $L$ , its inverse  $L^{-1}$  is compact by assumption and, therefore, the spectra of  $L^{-1}$  and of  $L_h^{-1}$  are bounded subsets of the intervals  $J := [0, \lambda_{\min}^{-1}]$  and  $J_h := [\lambda_{\max,h}^{-1}, \lambda_{\min,h}^{-1}] \subset J$ , respectively. Here,  $\lambda_{\min}, \lambda_{\min,h} > 0$  are the smallest eigenvalues of  $L$  and  $L_h$ , respectively, and again  $\lambda_{\max,h}$  denotes the largest eigenvalue of  $L_h$ . This motivates to consider a rational approximation  $r$  of the function  $f(x) := x^\beta$  on  $J$ . One can then deduce the non-fractional equation (3.4) for  $u_{h,m}^R$  from  $u_{h,m}^R = r(L_h^{-1})\mathcal{W}_h$ .

However, any rational approximation of  $f$  of the form

$$f(x) \approx \frac{\sum_{i=0}^{m_1} \tilde{c}_i x^i}{\sum_{j=0}^{m_2} \tilde{b}_j x^j}$$

would (after expanding the fraction with  $x^{m_*}$ ) yield a rational approximation,

$$x^{-\beta} = f(x^{-1}) \approx \frac{\sum_{i=0}^{m_1} \tilde{c}_i x^{m_*-i}}{\sum_{j=0}^{m_2} \tilde{b}_j x^{m_*-j}},$$

where the degree of the polynomials is  $m_* := \max\{m_1, m_2\}$  for both the numerator and the denominator, which conflicts with the choice (3.6) of different degrees  $m_\ell$  and  $m_r$ . For this reason, we decompose  $f$  via  $f(x) = \hat{f}(x)x^{m_\beta}$ , where we let  $\hat{f}(x) := x^{\beta-m_\beta}$ . We then approximate  $\hat{f} \approx \hat{r} := \frac{q_1}{q_2}$  on  $J_h$ , where  $q_1(x) := \sum_{i=0}^m c_i x^i$  and  $q_2(x) := \sum_{j=0}^{m+1} b_j x^j$  are polynomials of degree  $m$  and  $m+1$ , respectively. The

function  $r(x) := \hat{r}(x)x^{m_\beta}$  is then an approximation of  $f$ . This construction leads (after expanding the fraction with  $x^m$ ) to a rational approximation  $\frac{p_r}{p_\ell}$  of  $x^{-\beta}$ :

$$x^{-\beta} = f(x^{-1}) \approx \hat{r}(x^{-1})x^{-m_\beta} = \frac{q_1(x^{-1})}{q_2(x^{-1})x^{m_\beta}} = \frac{\sum_{i=0}^m c_i x^{m-i}}{\sum_{j=0}^{m+1} b_j x^{m+m_\beta-j}}. \quad (3.7)$$

Thus, we choose  $p_\ell(x) := \sum_{j=0}^{m+1} b_j x^{m+m_\beta-j}$  of degree  $m + m_\beta$  as well as  $p_r(x) := \sum_{i=0}^m c_i x^{m-i}$  of degree  $m$ , and we define  $P_{\ell,h}$ ,  $P_{r,h}$  in (3.4) accordingly,

$$P_{\ell,h} := p_\ell(L_h) = \sum_{j=0}^{m+1} b_j L_h^{m+m_\beta-j}, \quad P_{r,h} := p_r(L_h) = \sum_{i=0}^m c_i L_h^{m-i}. \quad (3.8)$$

Their continuous counterparts in (3.5) are  $P_\ell := p_\ell(L)$  and  $P_r := p_r(L)$ .

We note that, for (3.6) to hold, any choice  $m_2 \in \{0, 1, \dots, m + m_\beta\}$  would have been permissible for the polynomial degree of  $q_2$ , if  $m$  is the degree of  $q_1$ . The reason for setting  $m_2 = m + 1$  is that this is the maximal choice, which is universally applicable for all values of  $m_\beta \in \mathbb{N}$ .

In the following we refer to  $u_{h,m}^R$  in (3.4) with  $P_{\ell,h}$ ,  $P_{r,h}$  defined by (3.8) as the rational (SPDE) approximation of degree  $m$ . We emphasize that this approximation relies (besides the finite element discretization in space) only on the rational approximation of the function  $\hat{f}$ . In particular, no information about the operator  $L$  except for a lower bound of the eigenvalues is needed. In the Matérn case, we have  $L = \kappa^2 - \Delta$  and an obvious lower bound of the eigenvalues is therefore given by  $\kappa^2$ . To improve the stability of the method, we will rescale the operator so that the lower bound is equal to one, which for the Matérn case corresponds to reformulating the SPDE (1.3) as  $(\text{Id} - \kappa^{-2}\Delta)^\beta(\tilde{\tau}u) = \mathcal{W}$ , where  $\tilde{\tau} := \kappa^{2\beta}\tau$ , and using  $L = \text{Id} - \kappa^{-2}\Delta$ .

**3.3. An error bound for the rational approximation.** In this section we justify the approach presented in §3.2 by providing an upper bound for the strong mean-square error  $\|u - u_{h,m}^R\|_{L_2(\Omega; L_2(\mathcal{D}))}$ . Here  $u$  and  $u_{h,m}^R$  are the solutions of (1.2) and (3.4) and the rational approximation  $u_{h,m}^R$  is constructed as described in §3.2, assuming that  $\hat{r} = \hat{r}_h$  is the  $L_\infty$ -best rational approximation of  $\hat{f}(x) = x^{\beta-m_\beta}$  on the interval  $J_h$  for each  $h$ . This means that the resulting approximation minimizes the error in the supremum norm on  $J_h$  among all rational approximations of the chosen degrees in numerator and denominator. How such approximations can be computed is discussed in §3.4.

The theoretical analysis for this case, presented in Appendix B, results in the following theorem, showing strong convergence of the rational approximation  $u_{h,m}^R$  to the exact solution  $u$ .

**Theorem 3.3.** *Let  $u$ ,  $u_{h,m}^R$  be the solutions to (1.2) and (3.4), respectively. Under the above assumptions, there exists a constant  $C > 0$ , independent of  $h$  and  $m$ , such that, for sufficiently small  $h$ ,*

$$\|u - u_{h,m}^R\|_{L_2(\Omega; L_2(\mathcal{D}))} \leq C \left( h^{\min\{d(\alpha\beta-1/2), p+1\}} + h^{\min\{d\alpha(\beta-1), 0\} - d/2} e^{-2\pi\sqrt{|\beta-m_\beta|m}} \right).$$



TABLE 1. Coefficients of the rational approximation for  $\beta = 3/4$  (exponential covariance on  $\mathbb{R}^2$ ) for  $m = 1, 2, 3, 4$ , normalized so that  $c_m = 1$ .

$m$		$j = 0$	$j = 1$	$j = 2$	$j = 3$	$j = 4$	$j = 5$
1	$c_j$	7.6905e-2	1				
	$b_j$	1.6886e-2	8.0641e-1	2.5696e-1			
2	$c_j$	5.3014e-3	4.0512e-1	1			
	$b_j$	8.0794e-4	1.9789e-1	1.0712	1.4067e-01		
3	$c_j$	3.2738e-4	8.5667e-2	1.0034	1		
	$b_j$	3.7203e-5	3.0316e-2	6.8395e-1	1.2835	9.1664e-02	
4	$c_j$	1.8830e-5	1.3060e-2	4.4543e-1	1.8779	1	
	$b_j$	1.6560e-6	3.6170e-3	2.2788e-1	1.5729	1.4663	6.5651e-02

*Remark 3.4.* In order to calibrate the accuracy of the rational approximation with the finite element error, one can choose  $m \in \mathbb{N}$  such that

$$e^{-2\pi\sqrt{|\beta-m_\beta|m}} \propto h^{d\alpha \max\{\beta,1\}}.$$

The strong rate of mean-square convergence is then  $\min\{d(\alpha\beta - 1/2), p + 1\}$ . In the Matérn case, we would choose  $e^{-2\pi\sqrt{|\beta-m_\beta|m}} \propto h^{2 \max\{\beta,1\}}$  to obtain the strong convergence rate  $\min\{2\beta - d/2, p + 1\}$ .

**3.4. Computing the coefficients of the rational approximation.** As explained in §3.2, the coefficients  $\{c_i\}$  and  $\{b_j\}$  needed for defining the operators  $P_{\ell,h}$ ,  $P_{r,h}$  in (3.8) are obtained from a rational approximation  $\hat{r} = \hat{r}_h$  of  $\hat{f}(x) = x^{\beta-m_\beta}$  on  $J_h$ . For each  $h$ , this approximation can, e.g., be computed with the second Remez algorithm (Remez, 1934), which generates the coefficients of the  $L_\infty$ -best approximation. The error analysis for the resulting approximation  $u_{h,m}^R$  in (3.4) was performed in §3.3.

Despite the theoretical benefit of generating the  $L_\infty$ -best approximation, the Remez algorithm is often unstable in computations and, therefore, we use a different method in our simulations. However, versions of the Remez scheme were used, e.g., by Harizanov et al. (2016). A simpler and computationally more stable way of choosing the rational approximation is for instance the Clenshaw–Lord Chebyshev–Padé algorithm (Baker and Graves-Morris, 1996).

In order to avoid computing a different rational approximation  $\hat{r}$  for each finite element mesh size  $h$ , in practice we compute the approximation  $\hat{r}$  only once on the interval  $J_* := [\delta, 1]$ , where  $\delta \in (0, 1)$  should ideally be chosen such that  $J_h \subset J_*$  for all considered mesh sizes  $h$ . For the numerical experiments later, we will use  $\delta = 10^{-(5+m)/2}$  when computing rational approximations of order  $m$ , which gives acceptable results for all values of  $\beta$ . As an example, the resulting coefficients computed with the Clenshaw–Lord Chebyshev–Padé algorithm on  $J_*$  for the case of exponential covariance on  $\mathbb{R}^2$  (i.e.,  $\beta = 3/4$ ) are shown in Table 1.

#### 4. COMPUTATIONAL ASPECTS OF THE RATIONAL APPROXIMATION

In the non-fractional case, the sparsity of the precision matrix for the weights  $\mathbf{u}$  in (1.1) facilitates fast computation of samples, likelihoods, and other quantities of

interest for statistical inference. The purpose of this section is to show that the rational SPDE approximation proposed in §3 preserves these good computational properties.

The key observation for using the rational SPDE approximation for inference is that the operators  $P_\ell$  and  $P_r$  are commutative by construction. We can thus rewrite the model  $P_\ell u = P_r \mathcal{W}$  as

$$\begin{aligned} P_\ell x &= \mathcal{W} & \text{in } \mathcal{D}, \\ u &= P_r x & \text{in } \mathcal{D}. \end{aligned} \quad (4.1)$$

This representation shows that the model can be seen as a Markov random field transformed by the differential operator  $P_r$ , which is a particular case of the nested SPDE models that have been studied by Bolin and Lindgren (2011).

Discretizing this latent model by means of a FEM with basis functions  $\{\varphi_j\}_{j=1}^n$ , as explained in Appendix A, yields an approximation of the form (1.1), where  $\Sigma_u = \mathbf{P}_r \mathbf{Q}^{-1} \mathbf{P}_r^\top$ . Here  $\mathbf{P}_\ell, \mathbf{P}_r \in \mathbb{R}^{n \times n}$  correspond to the discrete operators  $P_{\ell,h}$  and  $P_{r,h}$ , respectively, and  $\mathbf{Q} := \mathbf{P}_\ell^\top \mathbf{C}^{-1} \mathbf{P}_\ell$  is sparse if the mass matrix  $\mathbf{C}$  with respect to the finite element basis  $\{\varphi_j\}_{j=1}^n$  is replaced by the diagonal lumped mass matrix  $\tilde{\mathbf{C}}$ , see Appendix A. By defining  $\mathbf{x} \sim \mathbf{N}(\mathbf{0}, \mathbf{Q}^{-1})$ , we have  $\mathbf{u} = \mathbf{P}_r \mathbf{x}$ , which is a transformed Gaussian Markov random field (GMRF). Choosing  $\mathbf{x}$  as a latent variable instead of  $\mathbf{u}$  thus enables us to use all computational methods, which are available for GMRFs (see Rue and Held, 2005), also for the rational SPDE approximation.

As an illustration, we consider the following hierarchical model, with a latent field  $u$  which is a rational approximation of (1.2),

$$\begin{aligned} y_i &= u(\mathbf{s}_i) + \varepsilon_i, & i = 1, \dots, N, \\ P_\ell u &= P_r \mathcal{W} & \text{in } \mathcal{D}, \end{aligned} \quad (4.2)$$

where  $u$  is observed under i.i.d. Gaussian measurement noise  $\varepsilon_i \sim \mathbf{N}(0, \sigma^2)$ . Given that one can treat this case, one can easily adapt the method to be used for inference in combination with MCMC or INLA (Rue et al., 2009) for models with more sophisticated likelihoods.

Defining the matrix  $\mathbf{A}$  with elements  $A_{ij} = \varphi_j(\mathbf{s}_i)$  and introducing the vector  $\mathbf{y} = (y_1, \dots, y_N)^\top$  gives us the discretized model

$$\begin{aligned} \mathbf{y} | \mathbf{x} &\sim \mathbf{N}(\mathbf{A} \mathbf{P}_r \mathbf{x}, \sigma^2 \mathbf{I}), \\ \mathbf{x} &\sim \mathbf{N}(\mathbf{0}, \mathbf{Q}^{-1}). \end{aligned} \quad (4.3)$$

In this way, the problem has been reduced to a standard latent GMRF model and a sparse Cholesky factorization of  $\mathbf{Q}$  can be used for sampling  $\mathbf{x}$  from  $\pi_x$  as well as to evaluate  $\log \pi_x(\mathbf{x})$ . Samples of  $\mathbf{u}$  can then be obtained from samples of  $\mathbf{x}$  via  $\mathbf{u} = \mathbf{P}_r \mathbf{x}$ . For evaluating  $\log \pi_u(\mathbf{u})$  one can use the relation  $\log \pi_u(\mathbf{u}) = \log \pi_x(\mathbf{P}_r^{-1} \mathbf{u})$ . Furthermore, the posterior distribution of  $\mathbf{x}$  is  $\mathbf{x} | \mathbf{y} \sim \mathbf{N}(\boldsymbol{\mu}_{x|y}, \mathbf{Q}_{x|y}^{-1})$ , where  $\boldsymbol{\mu}_{x|y} = \sigma^{-2} \mathbf{Q}_{x|y}^{-1} \mathbf{P}_r^\top \mathbf{A}^\top \mathbf{y}$  and  $\mathbf{Q}_{x|y} = \mathbf{Q} + \sigma^{-2} \mathbf{P}_r^\top \mathbf{A}^\top \mathbf{A} \mathbf{P}_r$  is a sparse matrix. Thus, simulations from  $\pi_{x|y}$  and evaluations of  $\log \pi_{x|y}(\mathbf{x})$  can be performed efficiently via a sparse Cholesky factorization of  $\mathbf{Q}_{x|y}$ . Finally, the marginal data log-likelihood is proportional to

$$\log |\mathbf{P}_\ell| - \frac{1}{2} \log |\mathbf{Q}_{x|y}| - N \log \sigma - \frac{1}{2} \left( \boldsymbol{\mu}_{x|y}^\top \mathbf{Q}_{x|y} \boldsymbol{\mu}_{x|y} + \sigma^{-2} \|\mathbf{y} - \mathbf{A} \mathbf{P}_r \boldsymbol{\mu}_{x|y}\|^2 \right).$$

We therefore conclude that all computations needed for statistical inference can be facilitated by sparse Cholesky factorizations of  $\mathbf{P}_\ell$  and  $\mathbf{Q}_{x|y}$ .

*Remark 4.1.* From the specific form of the matrices  $\mathbf{P}_\ell$  and  $\mathbf{P}_r$  addressed in Appendix A, we can deduce that the number of non-zero elements in  $\mathbf{Q}_{x|y}$  for a rational SPDE approximation of degree  $m$  will be the same as the number of non-zero elements in  $\mathbf{Q}_{x|y}$  for the standard (non-fractional) SPDE approach with  $\beta = m + m_\beta$ . Thus, also the computational cost will be comparable for these two cases.

## 5. NUMERICAL EXPERIMENTS

**5.1. The Matérn covariance on  $\mathbb{R}^2$ .** As a first test, we investigate the performance of rational SPDE approach for Gaussian Matérn fields, without including the finite element discretization in space.

The spectral density  $S$  of the solution to (1.3) on  $\mathbb{R}^2$  is given by (2.1), whereas the spectral density for the non-discretized rational SPDE approximation  $u_m^R$  in (3.5) is

$$S_R(\mathbf{k}) \propto \kappa^{4\beta} \left( \frac{\sum_{i=1}^m c_i (1 + \kappa^{-2} \|\mathbf{k}\|^2)^{m-i}}{\sum_{j=1}^{m+1} b_j (1 + \kappa^{-2} \|\mathbf{k}\|^2)^{m+m_\beta-j}} \right)^2. \quad (5.1)$$

We compute the coefficients as described in §3.4. For this purpose, we apply an implementation of the Clenshaw–Lord Chebyshev–Padé algorithm provided by the Matlab package Chebfun (Driscoll et al., 2014). Using a partial fraction decomposition of (5.1), expanding the square, transforming to polar coordinates, and using the fact that

$$\int_0^\infty \frac{\omega J_0(\omega h)}{(\omega^2 + a^2)(\omega^2 + b^2)} d\omega = \frac{1}{(b^2 - a^2)} (K_0(ah) - K_0(bh))$$

allows us to compute the corresponding covariance function  $C_R(h)$  analytically. Here,  $J_0$  is a Bessel function of the first kind and  $K_0$  is a modified Bessel function of the second kind. To measure the accuracy of the approximation, we compare  $C_R(h)$  to the true Matérn covariance function  $C(h)$  for different values of  $\nu$ , where  $\kappa = \sqrt{8\nu}$  is chosen such that the practical correlation range equals one in all cases.

The two top panels of Figure 1 show the results for the case of exponential covariance (i.e.,  $\nu = 1/2$  and  $\beta = 3/4$ ) using  $m = 1, 2, 3, 4$  for the degree of the rational approximation. To put the accuracy of the rational approximation in context, the Markov approximation by Lindgren et al. (2011) as well as the quadrature method by Bolin et al. (2017) are also shown. For the quadrature method,  $K = 12$  quadrature nodes are used, which results in an approximation with the same computational cost as a rational approximation of degree  $m = 11$ , see Appendix C. The two bottom panels show the normalized error in the  $L_2$ -norm and the error with respect to  $L_\infty$ -norm, both with respect to the interval  $[0, 2]$  of length twice the practical correlation range, i.e.,

$$\left( \frac{\int_0^2 (C(h) - C_a(h))^2 dh}{\int_0^2 C(h)^2 dh} \right)^{1/2} \quad \text{and} \quad \sup_{h \in [0, 2]} |C(h) - C_a(h)|$$

for different values of  $\nu$ , where  $C_a$  is the covariance function obtained by the respective approximation method.

Already for  $m = 3$ , the rational approximation performs better than both the Markov approximation and the quadrature approximation for all values of  $\nu$ . It

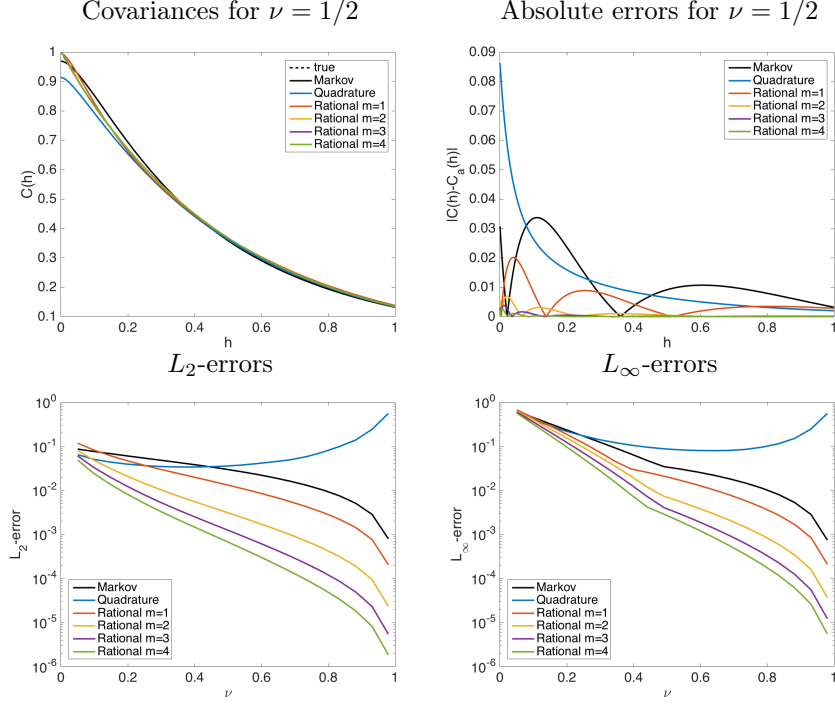


FIGURE 1. Results for the rational and Markov approximations when  $\kappa = \sqrt{8\nu}$ .

also decreases the error for the case of an exponential covariance by several orders of magnitude. Furthermore, as can be seen in Figure 2, the approximations are even more accurate for  $\nu > 1$ .

It should be noted that the performance of the quadrature method can be improved by increasing the number of quadrature nodes, see Appendix C. This is reasonable if the method is needed only for sampling from the model, but implementing this method for statistical applications, which require kriging or likelihood evaluations, is not feasible since the computational costs then are comparable to the standard SPDE approach with  $\beta = K$ .

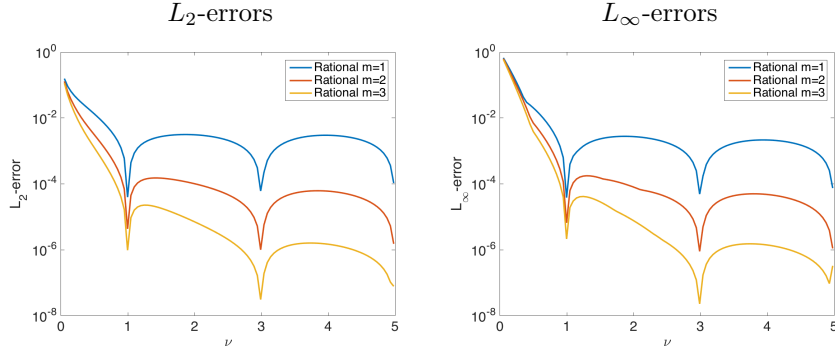


FIGURE 2.  $L_2$ - and  $L_\infty$ -errors of the rational approximation for different values of  $\nu$ .

**5.2. Computational cost and the finite element error.** From the study in the previous subsection, we infer that the rational SPDE approach performs well for Matérn fields with arbitrary smoothness. However, as for the standard SPDE approach, we need to discretize the problem to be able to use the method in practice, e.g., for inference. This induces an additional error source, which means that one should balance the two errors by choosing the degree  $m$  of the rational approximation appropriately with respect to the FEM error. This was done in theory in Remark 3.4. In this section we address this issue in practice and investigate the computational cost of the rational SPDE approximation.

As a test case, we compute approximations of a Gaussian Matérn field with unit variance and practical correlation range  $r = 0.1$  on the unit square in  $\mathbb{R}^2$ . We assume homogeneous Neumann boundary conditions for the Matérn operator  $\kappa^2 - \Delta$  in (1.3). For the discretization, we use a FEM with a nodal basis of continuous piecewise linear functions with respect to a mesh induced by a Delaunay triangulation of a regular lattice on the domain, with a total of  $n$  nodes. The FEM error depends on the diameter  $h$  of the largest triangle in the mesh. We consider three different meshes with  $n = 57^2, 85^2, 115^2$ , which corresponds to  $h \approx r/4, r/6, r/8$ . In order to measure the accuracy of the method, we compute the covariance between the midpoint of the domain  $\tilde{\mathbf{s}}_*$  and all other nodes in the lattice  $\{\tilde{\mathbf{s}}_j\}_{j=1}^n$  for the Matérn field and the rational SPDE approximations and calculate the error similarly to the normalized  $L_2$ -error in §5.1,

$$\left( \frac{\sum_{j=1}^n (C(\delta_j) - \Sigma_{j,*}^{\mathbf{u}})^2}{\sum_{j=1}^n C(\delta_j)^2} \right)^{1/2},$$

where  $\delta_j := \|\tilde{\mathbf{s}}_* - \tilde{\mathbf{s}}_j\|$  and  $\Sigma^{\mathbf{u}} = \mathbf{P}_r \mathbf{P}_\ell^{-1} \mathbf{C} \mathbf{P}_\ell^{-\top} \mathbf{P}_r^\top$  is the covariance matrix of  $\mathbf{u}$ , see Appendix A. As measures of the computational cost, we consider the time it takes to sample  $\mathbf{u}$  and to evaluate  $\log |\mathbf{Q}_{x|y}|$  from the model (4.3) with  $\sigma = 1$ , when  $\mathbf{y}$  is a vector of noisy observations of the latent field at 1000 locations, drawn at random in the domain (a similar amount of time is needed to evaluate  $\boldsymbol{\mu}_{x|y}$ ).

The results for rational SPDE approximations of different degrees for the case  $\beta = 3/4$  (exponential covariance) are shown in Table 2. Furthermore, we perform the same experiment when the standard (non-fractional) SPDE approach is used for  $\beta = 2, 3$ . As previously mentioned in Remark 4.1, the computational cost of the rational SPDE approximation of degree  $m$  should be comparable to the standard SPDE approach with  $\beta = m + 1$ . Table 2 validates this claim. One can also note that the errors of the rational SPDE approximations are similar to those of the standard SPDE approach, and that the reduction in error when increasing from  $m = 2$  to  $m = 3$  is small for all cases, which indicates that the error induced by the rational approximation is small compared to the FEM error, even for a low degree  $m$ . This is also the reason for why, in particular in the pre-asymptotic region, one can in practice choose the degree  $m$  smaller than the value suggested in Remark 3.4, which gives  $m \approx 6, 7, 8$  for  $\beta = 3/4$  and the three considered finite element meshes.

**5.3. Likelihood-based inference of Matérn parameters.** The computationally efficient evaluation of the likelihood of the rational SPDE approximation facilitates likelihood-based inference for all parameters of the Matérn model, including  $\nu$

TABLE 2. Covariance errors and computing times for sampling from the rational SPDE approximation  $\mathbf{u}$  and evaluating  $\log |\mathbf{Q}_{x|y}|$ . For reference, the corresponding values for the standard SPDE approach with  $\beta = 2, 3$  are given.

$n$		Rational SPDE approximation			Reference	
		$m = 1$	$m = 2$	$m = 3$	$\beta = 2$	$\beta = 3$
$57^2$	Error	0.0185	0.0134	0.0141	0.0282	0.0279
	Sample	0.0171	0.0238	0.0367	0.0340	0.0561
	$\log  \mathbf{Q}_{x y} $	0.0369	0.0667	0.1127	0.0280	0.0454
$85^2$	Error	0.0172	0.0076	0.0081	0.0120	0.0120
	Sample	0.0425	0.0671	0.1044	0.0858	0.1538
	$\log  \mathbf{Q}_{x y} $	0.0837	0.1654	0.2885	0.0727	0.1419
$115^2$	Error	0.0156	0.0053	0.0050	0.0065	0.0065
	Sample	0.0863	0.1605	0.2556	0.1924	0.3764
	$\log  \mathbf{Q}_{x y} $	0.1819	0.3665	0.6741	0.1684	0.3299

which until now had to be fixed when using the SPDE approach. In this section we investigate the accuracy of this approach within the scope of a simulation study.

We again assume homogeneous Neumann boundary conditions for the Matérn operator in (1.3) and consider the standard latent model (4.2) from §4. We take the unit square as the domain of interest, set  $\sigma^2 = 0.1$ ,  $\nu = 0.5$  and choose  $\kappa$  and  $\tau$  so that the latent field has variance  $\phi = 1$  and practical correlation range 0.2. For the FEM, we take a mesh based on a regular lattice on the domain, extended by twice the correlation range in each direction to reduce boundary effects, yielding a mesh with approximately 3500 nodes.

As a first test case, we use simulated data from the discretized model. To make sure that the parameters are identifiable, we simulate 50 replicates of the latent field, each with corresponding noisy observations at 1000 measurement locations drawn at random in the domain. This results in a total of 50000 observations, which we use to estimate the parameters of the model. We draw initial values for the parameters at random and then numerically optimize the likelihood of the model with the function `fminunc` in Matlab. This procedure is repeated 100 times, each time with a new simulated data set.

As a second test case, we repeat the simulation study, but this time we simulate the data from a Gaussian Matérn field with an exponential covariance function instead of from the discretized model. For the estimation, we compute the rational SPDE approximation for the same finite element mesh as in the first test case. To investigate the effect of the mesh resolution on the parameter estimates, we also estimate the parameters using a uniformly refined mesh with twice as many nodes.

The results can be seen in Table 3, where the true parameter values are shown together with the mean and standard deviations of the 100 estimates for each case. Notably, we are able to estimate all parameters accurately in the first case. For the second case, the finite element discretization seems to induce a small bias, especially for the nugget estimate ( $\sigma^2$ ) that depends on the resolution of the mesh. The bias in the nugget estimate is not surprising since the increased nugget compensates for

TABLE 3. Results of the parameter estimation. For each parameter estimate, the mean of 100 different estimates is shown, with the corresponding standard deviation in parentheses.

		Rational samples		Matérn samples	
	Truth	Estimate		Coarse mesh	Fine mesh
$\kappa$	10	10.026	(0.5661)	10.966	(1.8060) 10.864 (0.4414)
$\phi$	1.0	1.0014	(0.0228)	1.1089	(0.6155) 0.9743 (0.0210)
$\sigma^2$	0.1	0.1001	(0.0009)	0.3016	(0.0036) 0.2320 (0.0044)
$\nu$	0.5	0.5011	(0.0168)	0.5554	(0.0991) 0.5462 (0.0138)

the FEM error. The bias could be decreased by choosing the mesh more carefully, also taking the measurement locations into account. In practice, however, this bias will not be of great importance, since the optimal nugget for the discretized model should be used, and not the optimal value for the corresponding exact model.

## 6. APPLICATION

In this section we illustrate how the rational SPDE approach can be used for spatial prediction and compare the accuracy of the method to that of covariance tapering. We consider the problem of interpolating the data set of standardized precipitation anomalies from (Furrer et al., 2006), which consists of  $N = 5909$  observations  $\mathbf{Y}$  for the conterminous U.S. for April 1948, and is shown in Figure 3. Furrer et al. (2006) proposed to model the data as observations of a Gaussian field  $u(\mathbf{s})$  with covariance function  $\phi_1 \exp(-h/\kappa_1) + \phi_2 \exp(-h/\kappa_2)$ , with variances  $\phi_1 = 0.277$ ,  $\phi_2 = 0.722$  and range parameters  $\kappa_1^{-1} = 40.73$ ,  $\kappa_2^{-1} = 523.73$ .

Based on this model, we aim at interpolating the data to a regular 0.25 degree lattice within the conterminous U.S., consisting of  $\hat{N} = 13083$  locations  $\hat{\mathbf{s}}_1, \dots, \hat{\mathbf{s}}_{\hat{N}}$ . Furrer et al. (2006) used covariance tapering, with a spherical correlation function with range 50 miles as a tapering function, to decrease the computational cost of the interpolation. Since the data set is relatively small, we can compute the optimal kriging predictor,  $\hat{u}(\mathbf{s}) = \mathbb{E}[u(\mathbf{s})|\mathbf{Y}]$ , and its corresponding variance

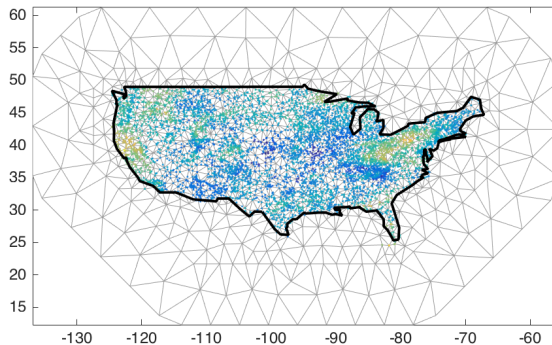


FIGURE 3. Data for the application and the mesh that is used for the FEM approximation.

TABLE 4. The errors (6.1) of the approximate kriging predictors compared to the result using the optimal kriging predictor and computation times using R (Matlab). A spherical taper was used in Matlab, whereas a Wendland taper was used in R.

	Optimal	Tapering	Rational
Err $_{\hat{u}}$	-	36.02 (27.94)	19.35 (19.30)
Err $_{\hat{\sigma}}$	-	71.77 (44.72)	38.39 (36.65)
Setup time	14.33 (9.40)	19.26 (2.05)	1.316 (1.59)
Kriging time	46.66 (0.88)	0.416 (0.39)	0.447 (0.12)
Total time	60.99 (10.28)	19.68 (2.43)	1.763 (1.71)

$\hat{\sigma}^2(\mathbf{s}) = \text{Var}(u(\mathbf{s})|\mathbf{Y})$ . To measure the accuracy of the prediction based on Gaussian random field with a tapered covariance function (or on a rational SPDE approximation)  $u_a(\mathbf{s})$ , we use the errors

$$\text{Err}_{\hat{u}} = \left( \sum_{i=1}^{\hat{N}} (\hat{u}(\hat{\mathbf{s}}_i) - \hat{u}_a(\hat{\mathbf{s}}_i))^2 \right)^{1/2}, \quad \text{Err}_{\hat{\sigma}} = \left( \sum_{i=1}^{\hat{N}} (\hat{\sigma}(\hat{\mathbf{s}}_i) - \hat{\sigma}_a(\hat{\mathbf{s}}_i))^2 \right)^{1/2}, \quad (6.1)$$

where  $\hat{u}_a(\mathbf{s}) = \mathbb{E}[u_a(\mathbf{s})|\mathbf{Y}]$  and  $\hat{\sigma}_a^2(\mathbf{s}) = \text{Var}(u_a(\mathbf{s})|\mathbf{Y})$ .

To compare the tapering approximation with the rational SPDE approximation, we note that we can write the Gaussian field as  $u_1(\mathbf{s}) + u_2(\mathbf{s})$ , where  $u_i(\mathbf{s})$  has covariance function  $\phi_i \exp(-h/\kappa_i)$  for  $i = 1, 2$ . We compute rational SPDE approximations of  $u_1(\mathbf{s})$  and  $u_2(\mathbf{s})$  for  $m = 1$ , using the finite element mesh shown in Figure 3, and assuming homogeneous Neumann boundary conditions. The mesh has 1549 nodes and was computed using the R package INLA (Lindgren and Rue, 2015). To facilitate using the computational methods from §4 for this model, we consider  $\mathbf{u}(\mathbf{s}) = [u_1(\mathbf{s}), u_2(\mathbf{s})]^T$  as the latent field and include a small nugget  $\sigma^2 = 10^{-3}$  to account for the discretization error.

The rational SPDE approximation was implemented in R using the rSPDE package, and the tapering method was implemented using the fields package (Nychka et al., 2015b) and a Wendland tapering function with range 50 miles. To avoid problems with comparing implementations using different software packages, we additionally implemented a Matlab version of the comparison, where we instead used a spherical taper function to test the effect that the choice of tapering function has on the results. The results for both implementations are shown in Table 4. The table shows the kriging errors and the total computation time for the different methods. The time is further divided into two steps, where the first consists of the construction of all matrices that are needed, and the second is the interpolation. For the optimal prediction and the tapering method, the first step constructs all requisite covariance matrices. For the rational SPDE approximation, the first step consists of creating the finite element mesh, computing the rational approximations  $\hat{f}_1$  and  $\hat{f}_2$ , and assembling all matrices that are needed.

One can note that the rational SPDE approach is faster and more accurate than the tapering method, both using R and Matlab, despite the fact that we had to double the dimension of the latent variable to use the method for this problem. The reason for the higher accuracy is that the covariance function of the rational SPDE approximation is more similar to the true covariance function compared to



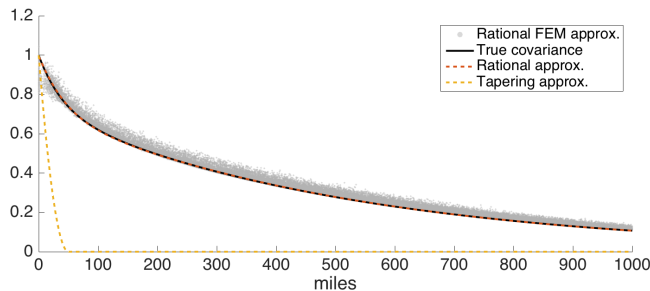


FIGURE 4. For the application, the true covariance function and the covariance functions for the tapering and the rational SPDE approximations (with and without the FEM error). For the rational SPDE approximation with FEM, the figure shows a random subsample of the covariances between the observation locations.

the tapering approximation, which is illustrated in Figure 4. The main source of error of the rational SPDE approximation stems from imposing Neumann boundary conditions. This increases the variance of the solution near the boundary. Thus, more accurate rational SPDE approximations could be obtained from extending the FEM mesh further outside the domain of interest.

## 7. DISCUSSION

We have introduced the rational SPDE approach providing a new type of computationally efficient approximations for a class of Gaussian random fields. These are based on an extension of the SPDE approach by Lindgren et al. (2011) to models with general fractional differential operators. An explicit rate of strong convergence for the method has been derived and we have shown how to calibrate the degree of the rational approximation with the mesh size of the FEM to achieve this rate.

Being able to use any fractional power opens up for using the SPDE approach for several new models, such as Gaussian fields with exponential covariances on  $\mathbb{R}^2$ . For the Matérn model and its extensions, it furthermore facilitates likelihood-based (or Bayesian) inference of all model parameters. For the sake of brevity, we have only illustrated how the method performs for approximating Matérn models, but it is applicable to many other models in statistics. A topic for future research is to use the rational SPDE approach for other fields which are difficult to approximate by GMRFs, such as models for data with long range dependence (Lilly et al., 2017) based on the fractional Brownian motion. The performance should then be compared to, e.g., approximations based on weighted sums of independent GMRFs. Such processes have been used to approximate both the fractional Brownian motion (Sørbye et al., 2017) and general Matérn fields (Nychka et al., 2015a).

Another topic for future research is to modify the fractional SPDE approach by replacing the FEM basis by a multiresolution basis and compare this approach to other multiresolution approaches such as (Katzfuss, 2017). Finally, it is also of interest to extend the method to non-Gaussian versions of the SPDE-based Matérn models (Bolin, 2014; Wallin and Bolin, 2015), since the Markov approximation considered by Wallin and Bolin (2015) is only computable under the restrictive requirement  $\beta \in \mathbb{N}$ .

## APPENDIX A. ITERATED FINITE ELEMENT METHOD

The rational approximation  $u_{h,m}^R$  of the solution  $u$  to (1.2) introduced in §3.2 is defined in terms of the discrete operators  $P_{\ell,h} = p_{\ell}(L_h)$  and  $P_{r,h} = p_r(L_h)$  via (3.4). Since the differential operator  $L$  in problem (1.2) is of second order, their continuous counterparts  $P_{\ell} = p_{\ell}(L)$  and  $P_r = p_r(L)$  in (3.5) are differential operators of order  $2(m + m_{\beta})$  and  $2m$ , respectively. Using a standard Galerkin approach for solving (3.5) would therefore require finite element basis functions  $\{\varphi_j\}$  in the Sobolev space  $H^{m+m_{\beta}}(\mathcal{D})$ , which are difficult to construct in more than one space dimension. This can be avoided by using a modified version of the iterated Hilbert space approximation method by Lindgren et al. (2011), and in this section we give the details of this procedure.

Recall from §3.1 that  $V_h \subset V$  is a finite element space with continuous piecewise polynomial basis functions  $\{\varphi_j\}_{j=1}^n$  of degree  $p \in \mathbb{N}$  defined with respect to a regular triangulation  $\mathcal{T}_h$  of the domain  $\mathcal{D}$  with mesh size  $h := \max_{T \in \mathcal{T}_h} \text{diam}(T)$ .

For computing the finite element approximation, we start by factorizing the polynomials  $q_1$  and  $q_2$  in the rational approximation  $\hat{r}$  of  $\hat{f}(x) = x^{\beta-m_{\beta}}$  in terms of their roots,

$$q_1(x) = \sum_{i=1}^m c_i x^i = c_m \prod_{i=1}^m (x - r_{1i}) \quad \text{and} \quad q_2(x) = \sum_{j=1}^{m+1} b_j x^j = b_{m+1} \prod_{j=1}^{m+1} (x - r_{2j}).$$

We use these expressions to reformulate (3.7) as

$$x^{-\beta} = f(x^{-1}) \approx \hat{r}(x^{-1})x^{-m_{\beta}} = \frac{c_m \prod_{i=1}^m (1 - r_{1i}x)}{b_{m+1}x^{m_{\beta}-1} \prod_{j=1}^{m+1} (1 - r_{2j}x)},$$

where, again, we have expanded the fraction with  $x^m$ . This representation shows that we can equivalently define the rational SPDE approximation  $u_{h,m}^R$  as the solution to (3.4) with  $P_{\ell,h}$ ,  $P_{r,h}$  redefined as

$$P_{\ell,h} = b_{m+1}L^{m_{\beta}-1} \prod_{j=1}^{m+1} (\text{Id} - r_{2j}L_h) \quad \text{and} \quad P_{r,h} = c_m \prod_{i=1}^m (\text{Id} - r_{1i}L_h).$$

We use the formulation of (3.4) as a system outlined in (4.1): We first solve  $P_{\ell,h}x_h = \mathcal{W}_h$  and use this approximation to compute the final approximation  $u_{h,m}^R = P_{r,h}x_h$ . In order to calculate  $x_h$ , we define for  $k \in \{1, \dots, m + m_{\beta}\}$  the functions  $x_k \in L_2(\Omega; V_h)$  iteratively by

$$\begin{aligned} b_{m+1}(\text{Id} - r_{21}L_h)x_1 &= \mathcal{W}_h, \\ (\text{Id} - r_{2k}L_h)x_k &= x_{k-1}, \quad k = 2, \dots, m+1, \\ L_h x_k &= x_{k-1}, \quad k = m+2, \dots, m+m_{\beta}, \end{aligned}$$

and note that  $x_{m+m_{\beta}} = x_h$ .

By expanding  $x_k = \sum_{j=1}^n x_{kj}\varphi_j$  with respect to the finite element basis, we find that the stochastic weights  $\mathbf{x}_k = (x_{k1}, \dots, x_{kn})^{\top}$  satisfy

$$\begin{aligned} \sum_{j=1}^n x_{1j}b_{m+1}\langle \varphi_i, (\text{Id} - r_{21}L)\varphi_j \rangle &= \langle \varphi_i, \mathcal{W}_h \rangle, \\ \sum_{j=1}^n x_{kj}\langle \varphi_i, (\text{Id} - r_{2k}L)\varphi_j \rangle &= \sum_{j=1}^n x_{k-1,j}\langle \varphi_i, \varphi_j \rangle_{L_2(\mathcal{D})}, \quad k = 2, \dots, m+1, \end{aligned}$$

$$\sum_{j=1}^n x_{kj} \langle \varphi_i, L\varphi_j \rangle = \sum_{j=1}^n x_{k-1,j} (\varphi_i, \varphi_j)_{L_2(\mathcal{D})}, \quad k = m+2, \dots, m+m_\beta,$$

where each of these equations holds for  $i = 1, \dots, n$ . Recall from §3 that  $\mathcal{W}_h$  is white noise in  $V_h$ . This yields the distribution  $(\langle \varphi_i, \mathcal{W}_h \rangle)_{i=1}^n \sim N(\mathbf{0}, \mathbf{C})$ , where  $\mathbf{C}$  is the mass matrix with elements  $C_{ij} = (\varphi_i, \varphi_j)_{L_2(\mathcal{D})}$  and, therefore,

$$\mathbf{x}_k \sim N(\mathbf{0}, \mathbf{P}_{\ell,k}^{-1} \mathbf{C} \mathbf{P}_{\ell,k}^{-\top}), \quad k = 1, \dots, m+m_\beta.$$

Here, the matrix  $\mathbf{P}_{\ell,k}$  is defined by

$$\mathbf{P}_{\ell,k} = \begin{cases} b_{m+1} \mathbf{C} \mathbf{L}_k, & 1 \leq k \leq m+1, \\ b_{m+1} \mathbf{C} (\mathbf{C}^{-1} \mathbf{L})^{k-m-1} \mathbf{L}_{m+1}, & m+2 \leq k \leq m+m_\beta, \end{cases}$$

where  $\mathbf{L}_k := \prod_{j=1}^k (\mathbf{I} - r_{2j} \mathbf{C}^{-1} \mathbf{L})$  and the entries of  $\mathbf{L}$  are given by  $L_{ij} = \langle L\varphi_i, \varphi_j \rangle$ . In particular, the weights  $\mathbf{x}$  of  $x_h$  have distribution

$$\mathbf{x} \sim N(\mathbf{0}, \mathbf{P}_\ell^{-1} \mathbf{C} \mathbf{P}_\ell^{-\top}), \quad \text{where } \mathbf{P}_\ell := \mathbf{P}_{\ell, m+m_\beta}. \quad (\text{A.1})$$

Note also that for the Matérn case  $L = \kappa^2 - \Delta$ , we have  $\mathbf{L} = \kappa^2 \mathbf{C} + \mathbf{G}$ , where  $\mathbf{G}$  is the stiffness matrix with elements  $G_{ij} = (\nabla \varphi_i, \nabla \varphi_j)_{L_2(\mathcal{D})}$ .

To obtain the final approximation, we calculate  $u_{h,m}^R = P_{r,h} x_h$  by using a similar iterative procedure. Let  $u_1, \dots, u_m$  be defined by

$$\begin{aligned} u_1 &= c_m (\text{Id} - r_{11} L_h) x_h, \\ u_k &= (\text{Id} - r_{1k} L_h) u_{k-1}, \quad k = 2, \dots, m. \end{aligned}$$

Then  $u_{h,m}^R = c_m (\prod_{i=1}^m (\text{Id} - r_{1i} L_h)) x_h = u_m$  and the weights  $\mathbf{u}_k$  of  $u_k$  are given in terms of the weights of  $x_h$  by

$$\mathbf{u}_k = \mathbf{P}_{r,k} \mathbf{x}, \quad \text{where } \mathbf{P}_{r,k} := c_m \prod_{i=1}^k (\mathbf{I} - r_{1i} \mathbf{C}^{-1} \mathbf{L}).$$

By (A.1), this implies that the distribution of the weights of the final rational approximation  $u_{h,m}^R$  is given by

$$\mathbf{u} \sim N(\mathbf{0}, \mathbf{P}_r \mathbf{P}_\ell^{-1} \mathbf{C} \mathbf{P}_\ell^{-\top} \mathbf{P}_r^\top), \quad \text{where } \mathbf{P}_r := \mathbf{P}_{r,m}.$$

To obtain sparse matrices  $\mathbf{P}_\ell$  and  $\mathbf{P}_r$ , we approximate the mass matrix  $\mathbf{C}$  by a diagonal matrix  $\tilde{\mathbf{C}}$  with diagonal elements  $\tilde{C}_{ii} = \sum_{j=1}^n C_{ij}$ . The effect of this ‘‘mass lumping’’ was motivated theoretically by Lindgren et al. (2011), and was empirically shown to be small by Bolin and Lindgren (2013).

## APPENDIX B. CONVERGENCE ANALYSIS

In this section we give the details of the convergence result stated in Theorem 3.3. As mentioned in §3.3, we choose  $\hat{r} = \hat{r}_h$  as the  $L_\infty$ -best rational approximation of  $\hat{f}(x) = x^{\beta-m_\beta}$  on the interval  $J_h$  for each  $h$ . We furthermore assume that the operator  $L$  is normalized such that  $\lambda_1 \geq 1$  and, thus,  $J_h \subset J \subset [0, 1]$ .

Recall that Proposition 3.1 provides a bound for  $\|u - u_h\|_{L_2(\Omega; L_2(\mathcal{D}))}$ . Therefore, it remains is to estimate the strong error between  $u_{h,m}^R$  and  $u_h$  induced by the rational approximation of  $f(x) = x^\beta$ . To this end, recall the construction of the rational approximation  $u_{h,m}^R$  in §3.2: We first decomposed  $f$  as  $f(x) = \hat{f}(x) x^{m_\beta}$ , where  $\hat{f}(x) = x^{\beta-m_\beta}$ , and then used a rational approximation  $\hat{r} = \frac{q_1}{q_2}$  of  $\hat{f}$  on the

interval  $J_h = [\lambda_{\max,h}^{-1}, \lambda_{\min,h}^{-1}]$  with  $q_1 \in \mathcal{P}^m(J_h)$  and  $q_2 \in \mathcal{P}^{m+1}(J_h)$  to define the approximation  $r(x) := \hat{r}(x)x^{m\beta}$  of  $f$ . Here,  $\mathcal{P}^m(J_h)$  denotes the set of polynomials  $q: J_h \rightarrow \mathbb{R}$  of degree  $\deg(q) = m$ . In the following, we assume that  $\hat{r} = \hat{r}_h$  is the best rational approximation of  $\hat{f}$  of this form, i.e.,

$$\|\hat{f} - \hat{r}_h\|_{C(J_h)} = \inf \left\{ \|\hat{f} - \hat{\rho}\|_{C(J_h)} : \hat{\rho} = \frac{q_1}{q_2}, q_1 \in \mathcal{P}^m(J_h), q_2 \in \mathcal{P}^{m+1}(J_h) \right\},$$

where  $\|g\|_{C(J)} := \sup_{x \in J} |g(x)|$ .

For the analysis, we treat the two cases  $\beta \in (0, 1)$  and  $\beta \geq 1$  separately. If  $\beta \geq 1$ , then  $\hat{\beta} := \beta - m_\beta \in [0, 1)$ . Thus, if  $\hat{r}_*$  denotes the best rational approximation of  $\hat{f}$  on the interval  $[0, 1]$ , Theorem 1 of Stahl (2003) gives the bound

$$\|\hat{f} - \hat{r}_h\|_{C(J_h)} \leq \sup_{x \in [0,1]} |\hat{f}(x) - \hat{r}_*(x)| \leq \hat{C} e^{-2\pi\sqrt{\hat{\beta}m}},$$

where the constant  $\hat{C} > 0$  is continuous in  $\hat{\beta}$  and independent of  $h$  and the degree  $m$ . Since  $x^{m\beta} \leq 1$  for all  $x \in J_h$ , we obtain for  $r_h(x) := \hat{r}_h(x)x^{m\beta}$  the same bound,

$$\|f - r_h\|_{C(J_h)} \leq \sup_{x \in J_h} |\hat{f}(x) - \hat{r}_h(x)| \leq \hat{C} e^{-2\pi\sqrt{\hat{\beta}m}}. \quad (\text{B.1})$$

If  $\beta \in (0, 1)$ , then  $\hat{\beta} \in (-1, 0)$  and we let  $\tilde{r}$  be the best approximation of  $\tilde{f}(x) := x^{|\hat{\beta}|}$  on  $[0, 1]$ . A rational approximation of  $\tilde{f}$  on the different interval  $\tilde{J}_h := [\lambda_{\min,h}, \lambda_{\max,h}]$  is given by  $\tilde{R}_h(\tilde{x}) := \lambda_{\max,h}^{|\hat{\beta}|} \tilde{r}(\lambda_{\max,h}^{-1} \tilde{x})$  with error

$$\sup_{\tilde{x} \in \tilde{J}_h} |\tilde{f}(\tilde{x}) - \tilde{R}_h(\tilde{x})| \leq \lambda_{\max,h}^{|\hat{\beta}|} \sup_{x \in [0,1]} |\tilde{f}(x) - \tilde{r}(x)| \leq \tilde{C} \lambda_{\max,h}^{|\hat{\beta}|} e^{-2\pi\sqrt{|\hat{\beta}|m}},$$

where the constant  $\tilde{C} > 0$  depends only on  $|\hat{\beta}|$ . On  $J_h = [\lambda_{\max,h}^{-1}, \lambda_{\min,h}^{-1}]$  the function  $\tilde{R}_h(x^{-1})$  is an approximation of  $\hat{f}(x) = x^{\hat{\beta}} = \tilde{f}(x^{-1})$  and

$$\begin{aligned} \|\hat{f} - \hat{r}_h\|_{C(J_h)} &\leq \sup_{x \in J_h} |\hat{f}(x) - \tilde{R}_h(x^{-1})| \\ &\leq \sup_{\tilde{x} \in \tilde{J}_h} |\tilde{f}(\tilde{x}) - \tilde{R}_h(\tilde{x})| \leq \tilde{C} \lambda_{\max,h}^{|\hat{\beta}|} e^{-2\pi\sqrt{|\hat{\beta}|m}}. \end{aligned}$$

Finally, we use again the estimate  $x^{m\beta} \leq 1$  on  $J_h$  to obtain

$$\|f - r_h\|_{C(J_h)} \leq \|\hat{f} - \hat{r}_h\|_{C(J_h)} \leq \tilde{C} \lambda_{\max,h}^{|\hat{\beta}|} e^{-2\pi\sqrt{|\hat{\beta}|m}}. \quad (\text{B.2})$$

Proposition 3.1 and the observations (B.1)–(B.2) above yield Theorem 3.3, which is proven below.

*Proof of Theorem 3.3.* By Proposition 3.1, it suffices to bound  $\mathbb{E}\|u_h - u_{h,m}^R\|_{L_2(\mathcal{D})}^2$ . To this end, let  $\mathcal{W}_h = \sum_{j=1}^n \xi_j e_{j,h}$  be a Karhunen–Loève expansion of the white noise in  $V_h$ , where  $\{e_{j,h}\}_{j=1}^n$  are the eigenvectors of  $L_h$ , which correspond to the eigenvalues  $\{\lambda_{j,h}\}_{j=1}^n$  and which are orthonormal in  $L_2(\mathcal{D})$ .

By construction and owing to boundedness and invertibility of  $L_h$ , we have for  $u_{h,m}^R$  in (3.4) that  $u_{h,m}^R = P_{\ell,h}^{-1} P_{r,h} \mathcal{W}_h = r_h(L_h^{-1}) \mathcal{W}_h$  and we estimate

$$\mathbb{E}\|u_h - u_{h,m}^R\|_{L_2(\mathcal{D})}^2 = \mathbb{E} \sum_{j=1}^n \xi_j^2 \left( \lambda_{j,h}^{-\beta} - r_h(\lambda_{j,h}^{-1}) \right)^2 \leq n \max_{1 \leq j \leq n} |\lambda_{j,h}^{-\beta} - r_h(\lambda_{j,h}^{-1})|^2.$$

By (B.1) and (B.2), we can bound the last term by

$$\max_{1 \leq j \leq n} |\lambda_{j,h}^{-\beta} - r_h(\lambda_{j,h}^{-1})| \leq \sup_{x \in J_h} |f(x) - r_h(x)| \lesssim \lambda_{n,h}^{\max\{(1-\beta), 0\}} e^{-2\pi\sqrt{|\beta-m_\beta|m}}.$$

Finally, we obtain  $\lambda_{n,h} \lesssim \lambda_n \lesssim n^\alpha$  from the growth condition (3.2) of the eigenvalues and  $n \lesssim h^{-d}$  from the quasi-uniformity of the mesh. Thus,

$$\mathbb{E} \|u_h - u_{h,m}^R\|_{L_2(\mathcal{D})}^2 \lesssim h^{-2d\alpha \max\{(1-\beta), 0\} - d} e^{-4\pi\sqrt{|\beta-m_\beta|m}},$$

which completes the proof of Theorem 3.3.  $\square$

### APPENDIX C. A COMPARISON TO THE QUADRATURE APPROACH

Bolin et al. (2017) proposed another method which can be applied to compute sample paths of the solution  $u$  to (1.2) numerically. The approach therein is to express the discretized equation (3.1) as  $L_h^{\tilde{\beta}} L_h^{[\beta]} u_h = \mathcal{W}_h$ , where  $\tilde{\beta} = \beta - [\beta] \in [0, 1)$ . Since  $L_h^{[\beta]} u_h = f$  can be solved by using non-fractional methods, the focus was on the case  $\beta \in (0, 1)$  when constructing the approximative solution. From the Dunford–Taylor calculus (Yosida, 1995, §IX.11) we have in this case the following representation of the discrete inverse,

$$L_h^{-\beta} = \frac{\sin(\pi\beta)}{\pi} \int_0^\infty \lambda^{-\beta} (\lambda \text{Id} + L_h)^{-1} d\lambda.$$

Bonito and Pasciak (2015) proposed a quadrature approximation  $Q_{h,k}^\beta$  of this integral after a change of variables  $\lambda = e^{-2y}$  and based on an equidistant grid  $\{y_\ell = \ell k : \ell = -K^-, \dots, K^+\}$  for  $y$  with step size  $k > 0$ , i.e.,

$$Q_{h,k}^\beta := \frac{2k \sin(\pi\beta)}{\pi} \sum_{\ell=-K^-}^{K^+} e^{2\beta y_\ell} (\text{Id} + e^{2y_\ell} L_h)^{-1}. \quad (\text{C.1})$$

Exponential convergence of order  $\mathcal{O}(e^{-\pi^2/(2k)})$  of the operator  $Q_{h,k}^\beta$  to the discrete fractional inverse  $L_h^{-\beta}$  was proven for

$$K^- := \left\lceil \frac{\pi^2}{4\beta k^2} \right\rceil \quad \text{and} \quad K^+ := \left\lceil \frac{\pi^2}{4(1-\beta)k^2} \right\rceil. \quad (\text{C.2})$$

By calibrating the number of quadrature nodes with the number of basis functions in the FEM, an explicit rate of convergence for the strong error of the approximation

$$u_{h,k}^Q = Q_{h,k}^\beta \mathcal{W}_h \quad \text{in } \mathcal{D}$$

was derived in (Bolin et al., 2017, Theorem 2.10). Motivated by the asymptotic convergence of the method, it was suggested to choose  $k \leq -\frac{\pi^2}{4\beta \ln(h)}$  for the Matérn case, in order to balance the errors induced by the quadrature and by a FEM of mesh size  $h$  (Table 1 of Bolin et al., 2017). This corresponds to a total number of  $K = K^- + K^+ + 1 > \frac{4\beta \ln(h)^2}{\pi^2(1-\beta)}$  quadrature nodes. The analogous asymptotic result for the degree  $m$  of the rational approximation  $u_{h,m}^R$  is given in Remark 3.4, suggesting the lower bound  $m \geq \frac{\ln(h)^2}{\pi^2(1-\beta)}$ , i.e.,  $K = 4\beta m$  asymptotically.

Furthermore, if we let  $c_\ell := e^{2y_\ell}$  and

$$P_{\ell,h}^Q := \prod_{\ell=-K^-}^{K^+} c_\ell^{-\beta} (\text{Id} + c_\ell L_h), \quad P_{r,h}^Q := \frac{2k \sin(\pi\beta)}{\pi} \sum_{j=-K^-}^{K^+} \prod_{\ell \neq j} c_\ell^{-\beta} (\text{Id} + c_\ell L_h),$$

we find that the quadrature-based approximation  $u_{h,k}^Q$  can equivalently be defined as the solution to the non-fractional SPDE

$$P_{\ell,h}^Q u_{h,k}^Q = P_{r,h}^Q \mathcal{W}_h \quad \text{in } \mathcal{D}. \quad (\text{C.3})$$

*Remark C.1.* A comparison of (C.3) with (3.4) shows that  $u_{h,k}^Q$  can be seen as a rational approximation of degree  $K^- + K^+$ , where the specific choice of the coefficients is implied by the quadrature. In combination with the remark above that  $K = 4\beta m$  quadrature nodes are needed to balance the errors, this shows that the computational cost for achieving a given accuracy with the rational approximation from §3.2 is lower than with the quadrature method, since  $\beta > d/4$ .

#### REFERENCES

- Baeumer, B., Kovács, M., and Sankaranarayanan, H. (2015). Higher order Grünwald approximations of fractional derivatives and fractional powers of operators. *Trans. Amer. Math. Soc.*, 367(2):813–834.
- Baker, G. A. and Graves-Morris, P. (1996). *Padé approximants*, volume 59. Cambridge University Press.
- Banerjee, S., Gelfand, A. E., Finley, A. O., and Sang, H. (2008). Gaussian predictive process models for large spatial data sets. *J. Roy. Statist. Soc. Ser. B Stat. Methodol.*, 70(4):825–848.
- Barbian, M. H. and Assunção, R. M. (2017). Spatial subsemble estimator for large geostatistical data. *Spatial Statistics*, 22:68–88.
- Bolin, D. (2014). Spatial Matérn fields driven by non-Gaussian noise. *Scand. J. Statist.*, 41:557–579.
- Bolin, D. (2017). rSPDE: Rational approximations of fractional spdes. R package version 0.1.0, <https://bitbucket.org/davidbolin/rspde>.
- Bolin, D., Kirchner, K., and Kovács, M. (2017). Numerical solution of fractional elliptic stochastic PDEs with spatial white noise. Preprint, arXiv:1705.06565.
- Bolin, D. and Lindgren, F. (2011). Spatial models generated by nested stochastic partial differential equations, with an application to global ozone mapping. *Ann. Appl. Statist.*, 5(1):523–550.
- Bolin, D. and Lindgren, F. (2013). A comparison between Markov approximations and other methods for large spatial data sets. *Comp. Stat. Data Anal.*, 61:7–21.
- Bonito, A., Lei, W., and Pasciak, J. E. (2017). The approximation of parabolic equations involving fractional powers of elliptic operators. *J. Comp. Appl. Math.*, 315:32–48.
- Bonito, A. and Pasciak, J. E. (2015). Numerical approximation of fractional powers of elliptic operators. *Math. Comp.*, 84(295):2083–2110.
- Caffarelli, L. and Silvestre, L. (2007). An extension problem related to the fractional Laplacian. *Comm. Partial Differential Equations*, 32(7-9):1245–1260.
- Cressie, N. and Johannesson, G. (2008). Fixed rank kriging for very large spatial data sets. *Journal of the Royal Statistical Society: Series B (Statistical Methodology)*, 70(1):209–226.

- Datta, A., Banerjee, S., Finley, A. O., and Gelfand, A. E. (2016). Hierarchical nearest-neighbor Gaussian process models for large geostatistical datasets. *Journal of the American Statistical Association*, 111(514):800–812.
- Driscoll, T. A., Hale, N., and Trefethen, L. N. (2014). Chebfun guide.
- Fuglstad, G.-A., Lindgren, F., Simpson, D., and Rue, H. (2015). Exploring a new class of non-stationary spatial gaussian random fields with varying local anisotropy. *Statistica Sinica*, 25:115–133.
- Furrer, R., Genton, M. G., and Nychka, D. (2006). Covariance tapering for interpolation of large spatial datasets. *J. Comput. Graph. Stat.*, 15(3):502–523.
- Gavrilyuk, I. P. (1996). An algorithmic representation of fractional powers of positive operators. *Numer. Funct. Anal. Optim.*, 17(3-4):293–305.
- Gavrilyuk, I. P., Hackbusch, W., and Khoromskij, B. N. (2004). Data-sparse approximation to the operator-valued functions of elliptic operator. *Math. Comp.*, 73(247):1297–1324.
- Gavrilyuk, I. P., Hackbusch, W., and Khoromskij, B. N. (2005). Hierarchical tensor-product approximation to the inverse and related operators for high-dimensional elliptic problems. *Computing*, 74(2):131–157.
- Harizanov, S., Lazarov, R., Marinov, P., Margenov, S., and Vutov, Y. (2016). Optimal solvers for linear systems with fractional powers of sparse SPD matrices. Preprint, arXiv:1612.04846.
- Heaton, M. J., Datta, A., Finley, A., Furrer, R., Guhaniyogi, R., Gerber, F., Gramacy, R. B., Hammerling, D., Katzfuss, M., Lindgren, F., et al. (2017). Methods for analyzing large spatial data: A review and comparison. *arXiv preprint arXiv:1710.05013*.
- Higdon, D. (2002). Space and space-time modeling using process convolutions. *Quantitative methods for current environmental issues*, 3754:37–56.
- Jin, B., Lazarov, R., Pasciak, J., and Rundell, W. (2015). Variational formulation of problems involving fractional order differential operators. *Math. Comp.*, 84(296):2665–2700.
- Katzfuss, M. (2017). A multi-resolution approximation for massive spatial datasets. *Journal of the American Statistical Association*, 112(517):201–214.
- Lilly, J. M., Sykulski, A. M., Early, J. J., and Olhede, S. C. (2017). Fractional Brownian motion, the Matérn process, and stochastic modeling of turbulent dispersion. *Nonlinear Process. Geophys.*, 24(3):481–514.
- Lindgren, F. and Rue, H. (2015). Bayesian spatial modelling with R-INLA. *J. Stat. Softw.*, 63(19):1–25.
- Lindgren, F., Rue, H., and Lindström, J. (2011). An explicit link between Gaussian fields and Gaussian Markov random fields: the stochastic partial differential equation approach (with discussion). *J. Roy. Statist. Soc. Ser. B Stat. Methodol.*, 73:423–498.
- Matérn, B. (1960). Spatial variation. *Meddelanden från statens skogsforskningsinstitut*, 49(5).
- Nochetto, R. H., Otárola, E., and Salgado, A. J. (2015). A PDE approach to fractional diffusion in general domains: a priori error analysis. *Found. Comp. Math.*, 15(3):733–791.
- Nychka, D., Bandyopadhyay, S., Hammerling, D., Lindgren, F., and Sain, S. (2015a). A multiresolution gaussian process model for the analysis of large spatial datasets. *J. Comput. Graph. Stat.*, 24(2):579–599.

- Nychka, D., Furrer, R., Paige, J., and Sain, S. (2015b). `fields`: Tools for spatial data. R package version 9.0.
- R Core Team (2017). *R: A Language and Environment for Statistical Computing*. R Foundation for Statistical Computing, Vienna, Austria.
- Remez, E. Y. (1934). Sur la détermination des polynômes d'approximation de degré donnée. *Comm. Soc. Math. Kharkov*, 10:41–63.
- Roininen, L., Lasanen, S., Orispää, M., and Särkkä, S. (2017). Sparse approximations of fractional Matérn fields. *Scand. J. Statist.*, pages n/a–n/a.
- Roop, J. P. (2006). Computational aspects of FEM approximation of fractional advection dispersion equations on bounded domains in  $\mathbb{R}^2$ . *J. Comput. Appl. Math.*, 193(1):243–268.
- Roazanov, J. A. (1977). Markov random fields and stochastic partial differential equations. *Sbornik: Mathematics*, 32(4):515–534.
- Rue, H. and Held, L. (2005). *Gaussian Markov Random Fields; Theory and Applications*, volume 104 of *Monographs on Statistics and Applied Probability*. Chapman & Hall/CRC, Boca Raton, FL.
- Rue, H., Martino, S., and Chopin, N. (2009). Approximate Bayesian inference for latent Gaussian models using integrated nested Laplace approximations (with discussion). *J. Roy. Statist. Soc. Ser. B Stat. Methodol.*, 71(2):319–392.
- Sang, H., Jun, M., and Huang, J. Z. (2011). Covariance approximation for large multivariate spatial data sets with an application to multiple climate model errors. *The Annals of Applied Statistics*, pages 2519–2548.
- Simpson, D., Lindgren, F., and Rue, H. (2012). In order to make spatial statistics computationally feasible, we need to forget about the covariance function. *Environmetrics*, 23(1):65–74.
- Sørbye, S. H., Myrvoll-Nilsen, E., and Rue, H. (2017). An approximate fractional gaussian noise model with  $O(n)$  computational cost. Preprint, arXiv:1709.06115.
- Stahl, H. R. (2003). Best uniform rational approximation of  $x^\alpha$  on  $[0, 1]$ . *Acta Math.*, 190(2):241–306.
- Wallin, J. and Bolin, D. (2015). Geostatistical modelling using non-Gaussian Matérn fields. *Scand. J. Statist.*, 42:872–890.
- Whittle, P. (1963). Stochastic processes in several dimensions. *Bull. Internat. Statist. Inst.*, 40:974–994.
- Yosida, K. (1995). *Functional Analysis*. Classics in Mathematics. Springer Berlin Heidelberg.